Journal of Electroceramics, 13, 707–713, 2004

Selective Gas Detection of SnO_2-TiO_2 Gas Sensors

WON JAE MOON, JI HAENG YU & GYEONG MAN CHOI

Department of Materials Science and Engineering, Pohang University of Science and Technology, San 31, Hyoja-dong, Pohang 790-784, South Korea

Submitted February 10, 2003; Revised November 6, 2003; Accepted November 18, 2003

Abstract. The composite, consisting of two materials with different sensing temperatures, may show the selectivity for a particular gas. In this study, the microstructural and compositional effects on the electrical conductivity and the CO and the H_2 gas sensing properties of SnO_2-TiO_2 composites were examined. SnO_2-TiO_2 composites in entire (0–100 mol%) composition range were fabricated in the form of porous pellet by sintering at 800°C for 3 h. The effects of CuO-coating (or doping) on the electrical conductivity and the sensing properties to 200 ppm CO and H_2 gases were examined.

With CuO-coating, SnO_2-TiO_2 composites showed the increased sensitivity to CO gas and a large difference in the sensing temperatures between CO and H_2 gases. As a result, CuO-coated SnO_2-TiO_2 composites showed the selectivity for CO gas between 100°C and 190°C and the selectivity for H_2 gas between 280°C and 380°C.

Keywords: SnO_2, TiO_2, CuO, composite, sensitivity, selectivity

1. Introduction

Semiconductor gas sensors have been researched for several decades owing to their advantages such as the low cost of fabrication, the high sensitivity, and the possibility of miniaturization and integration. *N*-type semiconductor materials such as SnO_2, ZnO, Fe_2O_3, and In_2O_3 have been used for the detection of inflammable or toxic gases such as NO_X, CH_4, or CO [1]. In order to improve the gas sensing properties of the sensors, many studies have been focused on the use of the noble metal catalysts [2] or the heterogeneous interface [3, 4]. However, they still lack the gas selectivity.

We have previously reported that SnO_2-ZnO [5] and SnO_2-Zn_2SnO_4 [6] composites coated with CuO showed the high selectivity to CO and H_2 gases at low and high temperatures, respectively. When the sensing materials are the composite of two phases that show good sensitivities at low (e.g., SnO_2) and high (e.g., ZnO or Zn_2SnO_4) temperature, respectively, the selective detection between CO and H_2 gases can be made. SnO_2-TiO_2 composites may be another candidate for the material with high CO selectivity due to the difference in sensing temperatures for SnO_2 (∼350°C) [7] and TiO_2 (above 400°C) [8, 9]. Thus, in this study, the electrical conductivity and the sensing properties of uncoated SnO_2-TiO_2 composites and CuO-coated SnO_2-TiO_2 composites to reducing gases (200 ppm CO and H_2 gases) were examined between 70°C and 560°C. The microstructural and compositional effects on the gas sensing properties, especially on the temperature (T_{MAX}) showing the maximum sensitivity values (S_{MAX}), were discussed.

2. Experimental Procedure

Appropriate amount of tin oxide powder (99.9%, Aldrich, USA) and titanium oxide powder (99.9%, anatase, Aldrich, USA) were mixed by ball milling in ethanol for 12 h. The slurry was filtered and dried. The mixed powders were uniaxially pressed into pellets and subsequently cold-isostatically pressed at 200 MPa. The pellets were sintered at 800°C for 3 h in air. The sintered densities of samples were measured by the Archimedean method. The phase and the microstructure were characterized by X-ray diffractometry

(XRD, MAC Science, M18XCE, JAPAN) and field-emission scanning-electron microscopy (FE-SEM, Hitachi, S-4200, JAPAN), respectively. The surface area of porous sintered pellet was determined by BET surface-area analyzer (Micromeritics, ASAP2010, USA).

For the CuO-coating, the sintered samples were dipped for 1 h in 1wt% CuO solution prepared by Pechini method [10]. The samples impregnated with CuO-solution were heated to 350°C for 2 h followed by firing at 750°C for 3 h. Provided that the pore of the samples was fully filled with the solution, the CuO content can be estimated as ∼0.2 mol% after firing. We found that the Cu was distributed homogeneously throughout the whole sample with CuO coating by using EPMA. Although the samples were coated with CuO, the effect of coating was previously found to be the same as the electrical doping [6]. Thus we have used the terms "coating" and "doping" interchangeably. Since CuO-coated SnO_2-TiO_2 composites were merely coated with CuO, the phase and the microstructure of the samples were expected to be unchanged from these of uncoated SnO_2-TiO_2 composite. Thus, we will refer the data of uncoated SnO_2-TiO_2 composite in the discussion related the microstructure information of CuO-coated SnO_2-TiO_2 composites.

For the measurement of electrical conductivity, the flat surfaces of the samples were painted with Pt paste (Engelhard model #6082, fluxed, USA) followed by firing at 600°C for 30 min. In order to exclude the moisture effect during the measurement procedure, the samples in a quartz tube were heated up to 560°C (uncoated system) or 440°C (coated system) in air and then cooled to the measurement temperature. The I-V characteristics were measured by using high-voltage source/measure unit (Keithley, K237, USA) after equilibrating the samples in air for 60 min. The applied voltage was varied from −10 to +10 volts. The current was measured 2 seconds after applying the voltage. The samples were kept in air for 30 min before changing the measurement temperature. The electrical measurement was repeated after flowing CO or H_2 gas, 200 ppm balanced by air, for 20 min at 100 cm^3/min rate. In order to eliminate the complication due to the water vapor effect, the relative humidity was fixed to 23% at 25°C by flowing the gases through the $MgCl_2$-saturated solution [11]. Gas sensitivity was defined as R_{Air}/R_{Gas}, where R_{Air} and R_{Gas} denote the electrical resistance values in air and in sample gas, respectively.

3. Results and Discussion

3.1. Phase and Microstructure

Figure 1 shows XRD patterns of SnO_2, ST10, ST99, and TiO_2 samples, sintered at 800°C for 3 h. The numbers in the sample notation represent TiO_2 mole fraction, for example, ST10 means 90 mol% SnO_2− 10 mol% TiO_2 sample. Although the SnO_2-TiO_2 system have the subsolidus miscibility gap [12], the crystal structures of SnO_2 and TiO_2 are the same, i.e., rutile. Thus the solubility limit of TiO_2 into SnO_2 and SnO_2 into TiO_2, respectively, was expected to be more than 10 mol% when sintered at 800°C. However, as shown by the small SnO_2 peaks in ST99 specimen, the solubility of SnO_2 into TiO_2 is estimated to be less than 1 mol% for the present study. On the other hand, TiO_2 peaks start to show up when more than 10 mol% TiO_2 was added into SnO_2. For the estimation of solubility limit of TiO_2 into SnO_2, the lattice parameters of SnO_2-rich phases were examined as shown in Fig. 2. As TiO_2 content increased, the lattice parameters of SnO_2-rich phases slightly decreased. However the decrease was

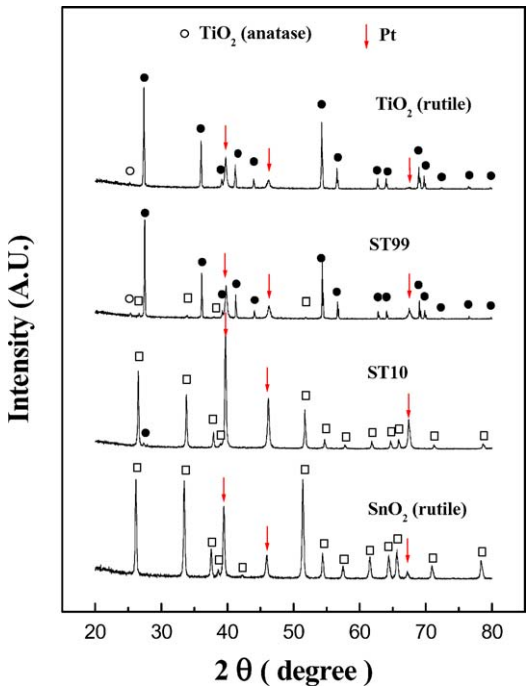

Fig. 1. XRD patterns of SnO_2, ST10, ST99, and TiO_2 samples sintered at 800°C for 3 h. Pt is reference phase for peak calibration.

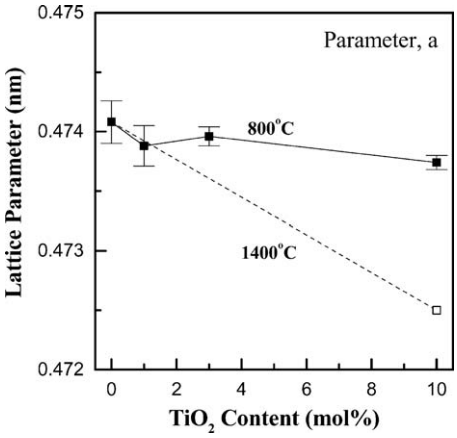

Fig. 2. The variation of lattice parameter a in SnO_2-rich phases. The solid line is for the samples sintered at 800°C for 3 h. The dashed line is the one expected for the powder calcined at 1400°C for 3 h.

very small compared with that of ST10 powder calcined at 1400°C for 3 h (dashed lines). In this study, to examine the equilibrium solubility, samples were also sintered at 1400°C. Samples sintered at 1400°C showed no second phase. Thus, the solubility of TiO_2 into porous SnO_2 at 800°C is estimated to be less than 2 mol% from this observation and SnO_2 and TiO_2 forms a mixture. This small solubility coincides with another phase diagram for SnO_2-TiO_2 shown by Garcia and Speidel [13] which shows very limited solubility of TiO_2 in SnO_2.

The fractured surfaces of the SnO_2-TiO_2 composite samples were shown in Fig. 3. All samples showed the relative sintered density of 60–65%. SnO_2 has much smaller particle size (<0.1 μm) than that of TiO_2 (~0.5 μm). As TiO_2 content increases in the composite, large TiO_2 particles start to show up. Up to 30 mol% TiO_2 content, the BET surface area of the samples increased from ~4.5 (SnO_2) to ~6.9 m^2/g (ST30). However, with further TiO_2 addition, the surface area of the composites continuously decreased. The maximum value of the surface area shown for ST30 sample is due possibly to the breakdown of agglomerated SnO_2 particles by TiO_2. Thus SnO_2 particles cover the surface of large TiO_2 particle as shown in Fig. 3.

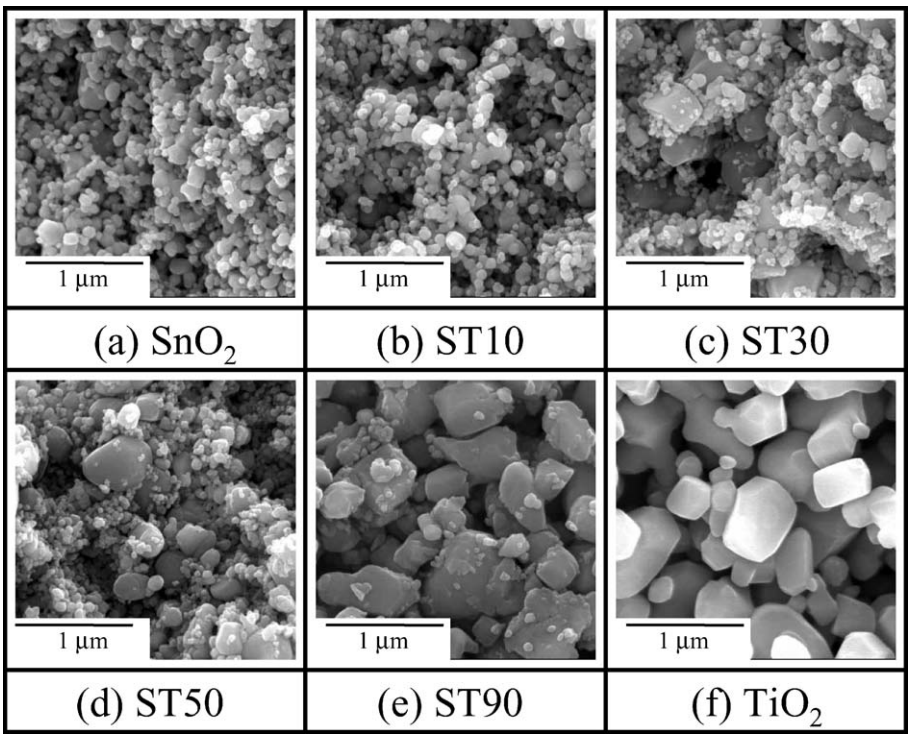

Fig. 3. FE-SEM micrographs of fractured surface of (a) SnO_2 (b) ST10, (c) ST30, (d) ST50, (e) ST90, and (f) TiO_2 samples.

3.2. Electrical and Gas Sensing Properties of Uncoated SnO_2-TiO_2 Composites

Figure 4 shows the electrical conductivity of SnO_2, TiO_2, and SnO_2-TiO_2 composites without Cu coating, plotted versus inverse of temperature in air (23% R.H.). All the samples examined in this study showed the nearly linear current-voltage (I-V) curves both in air and in reducing gases (200 ppm CO and 200 ppm H_2) and thus the electrical conductivity was calculated from the slope of I-V curve. SnO_2 showed the highest conductivity ($10^{-2.5}$–10^{-4} S/cm) among all samples. The electrical conductivity of SnO_2 continuously decreased with the increasing amount of TiO_2. Above 70 mol% TiO_2, the conductive values were mostly determined by the resistive TiO_2 phase. The conductive SnO_2-phase percolates the resistive TiO_2 matrix phase above ~30 mol% SnO_2. TiO_2-rich samples showed the conductivity minima at ~360°C due to the adsorption of water vapor. Water vapors are adsorbed with decreasing temperature.

Figure 5 shows the temperature dependence of the sensitivity of SnO_2, TiO_2, and SnO_2-TiO_2 composites to (a) 200 ppm CO and (b) 200 ppm H_2 gases. Note that the *y*-axis scales are different. SnO_2 showed the highest sensitivity value (~4) to CO gas at ~345°C. The addition of 10 mol% TiO_2 decreased the temperature showing the maximum sensitivity (T_{MAX}) for

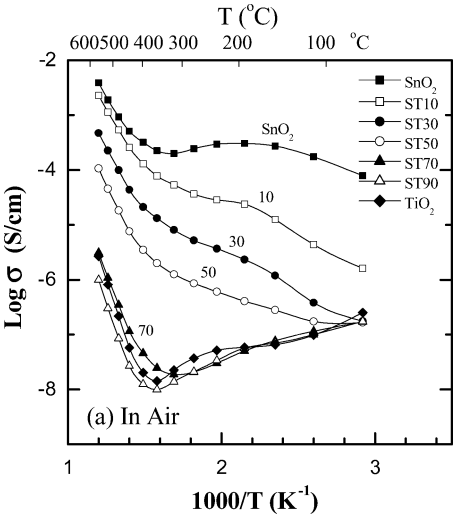

Fig. 4. Electrical conductivity of SnO_2, TiO_2, and uncoated SnO_2-TiO_2 composites in air (23% R.H.) plotted versus temperature. The numbers were included to help to identify the TiO_2 content.

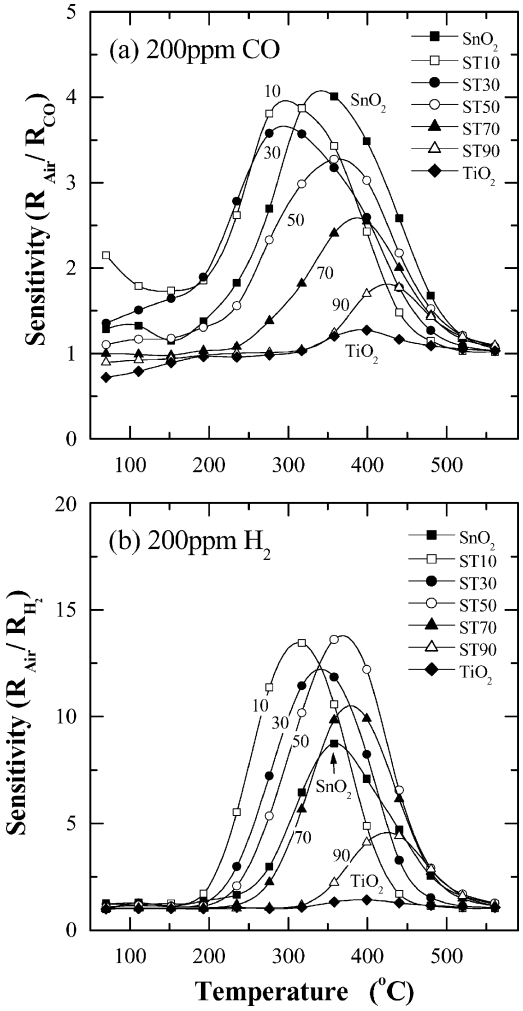

Fig. 5. Temperature dependence of the sensitivity to (a) 200 ppm CO and (b) 200 ppm H_2 gases of SnO_2, TiO_2, and uncoated SnO_2-TiO_2 composites.

CO gas as much as ~50°C from ~345 to ~295°C as shown in Fig. 5(a). However, the maximum sensitivity value (S_{MAX}) of ST10 sample to CO gas was not changed from that of SnO_2. Further addition of TiO_2 continuously decreased S_{MAX} to CO gas and shifted T_{MAX} toward higher temperature. Similarly, the T_{MAX} value of SnO_2 for H_2 gas also decreased as much as ~40°C from ~355 to ~315°C when 10 mol% TiO_2 was added as shown in Fig. 5(b) and then continuously increased above 10 mol% TiO_2. However, the S_{MAX} value to H_2 gas was much higher than that to CO gas. ST90 sample showed the maximum sensitivity values at ~430°C for both CO and H_2 gases. Thus it is evident

that TiO_2-rich phases have the higher T_{MAX} than that of SnO_2. The S_{MAX} of TiO_2 sample to both CO and H_2 gases showed less than 1.5 at ~400°C due to the large particle size (~0.5 μm). From the microstructural information shown in Fig. 3, the samples with composition between ST10 and ST50 were expected to show good sensitivity to reducing gases due to their fine particle sizes. The expectation was met in this study.

3.3. *Electrical and Gas Sensing Properties of CuO-Coated SnO_2-TiO_2 Composites*

Figure 6 shows the electrical conductivity of uncoated SnO_2, CuO-coated SnO_2 (SnO_2C) and TiO_2 (TiO_2C), and CuO-coated SnO_2-TiO_2 composites, plotted versus inverse of temperature in air (23% R.H.). The numbers in the sample notation represent TiO_2 mole fraction and 'C' indicates CuO-coating. For example, ST30C means 70 mol% SnO_2-30 mol% TiO_2 and CuO coated sample. In the previous section, Uncoated SnO_2 showed the highest conductivity ($10^{-4.1}$–$10^{-3.3}$S/cm) among all samples between 70 and 440°C. The electrical conductivity of SnO_2 drastically decreased with CuO coating, 1–4 orders of magnitude, depending upon temperature. In order to explain the reduced conductivity, the change of charge carriers in the bulk phase and surface should be considered. Since the particle size is not changed with CuO coating, the conductivity decrease is ascribed to the doping effect. When Cu^{+2} substitutes Sn^{+4}, the hole concentration increases and the conductivity of n-type SnO_2 decreases [7]. Thus, the reduced conductivity at high temperature, where the amount of the adsorbed oxygen ions is negligible, can be explained by doping effect. The CuO coated on the surface of SnO_2 particles may also boost oxygen adsorption, thus decreasing the conductivity of SnO_2. The electrical conductivity of composite continuously decreased with the increasing amount of TiO_2 due to the highly resistive TiO_2 phase. The CuO-coated SnO_2-TiO_2 composites showed approximately two orders of magnitude lower electrical conductivity than those for undoped SnO_2-TiO_2 composites.

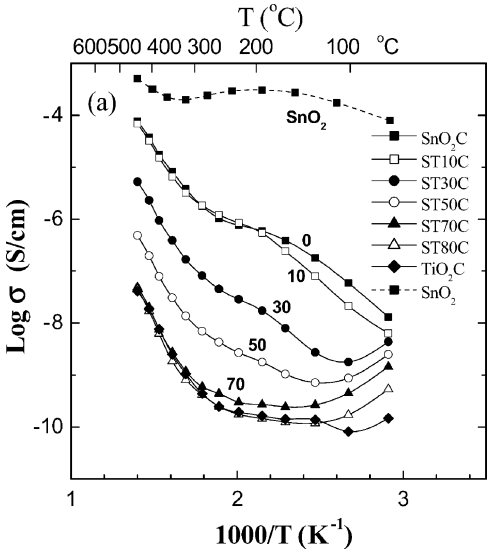

Fig. 6. Electrical conductivity of uncoated SnO_2, SnO_2C, TiO_2C, and CuO-coated SnO_2-TiO_2 composites in air (23% R.H.) plotted versus temperature. The numbers were included to help identifying the TiO_2 content.

Figure 7 shows the temperature dependence of the sensitivity of uncoated SnO_2, SnO_2C, TiO_2C, and CuO-coated SnO_2-TiO_2 composites to (a) 200 ppm CO and (b) 200 ppm H_2 gases. Note that the y-axis scales are different. The uncoated SnO_2 showed the maximum sensitivity (~4) to CO gas at ~345°C. With CuO coating or doping, the temperature showing the maximum sensitivity (T_{MAX}) for CO gas decreased from ~345 to ~255°C and the maximum sensitivity value (S_{MAX}) to CO gas increased from ~4 to ~8. The T_{MAX} value of SnO_2C for H_2 gas also decreased from ~355 to ~270°C with CuO coating as shown in Fig. 7(b). For SnO_2, the increase of S_{MAX} to H_2 gas due to CuO coating is much less in ratio than S_{MAX} to CO gas. We have previously reported that the addition of CuO also lowers T_{MAX} of ZnO [14] and SnO_2 [5]. CuO apparently acted as a catalyst and thus lowered T_{MAX} for CO and H_2 gases. Although SnO_2C showed the remarkably increased sensitivity only to CO gas, the difference in T_{MAX} to both gases was small. Thus, a low selectivity for CO gas was expected. The sensitivity values of TiO_2C sample to either CO or H_2 gas were less than 1.5 due to its large particle size. The sensitivity value of CuO-coated SnO_2-TiO_2 composites to CO gas did not change appreciably until TiO_2 was added above 50 mol%. In the previous section, when TiO_2 was added into SnO_2, the S_{MAX} to CO gas continuously decreased with TiO_2 content. For H_2 gas, the sensitivity value almost doubled from ~9.9 to ~18.3 when 30 mol% TiO_2 was added into SnO_2C. The increase of sensitivity value to H_2 gas was related to the increasing surface area with TiO_2 addition. Up to 50 mol% TiO_2, the sensitivity

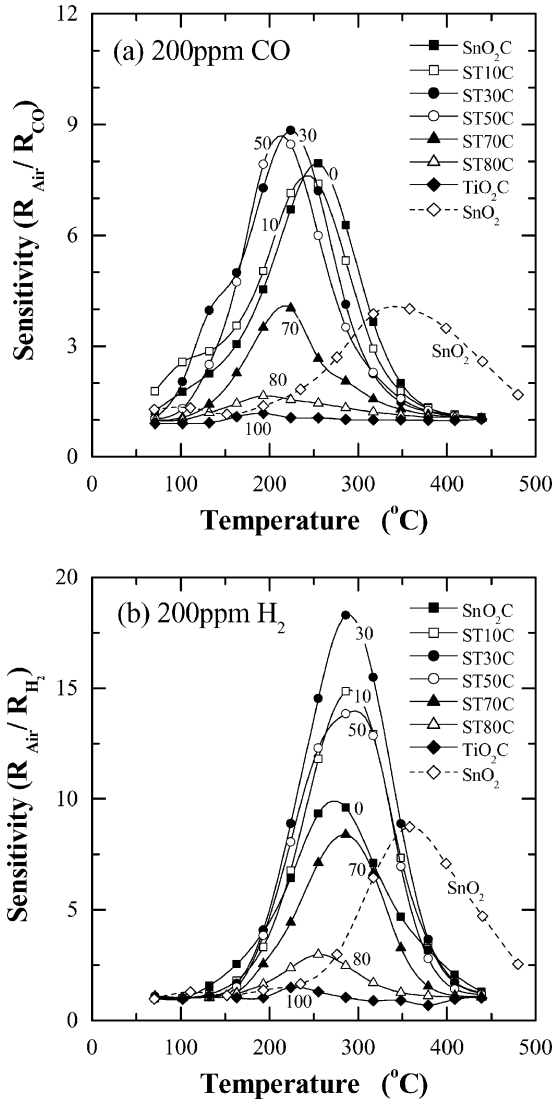

Fig. 7. Temperature dependence of the sensitivity to (a) 200 ppm CO and (b) 200 ppm H_2 gases of uncoated SnO_2, SnO_2C, TiO_2C, and CuO-coated SnO_2-TiO_2 composites.

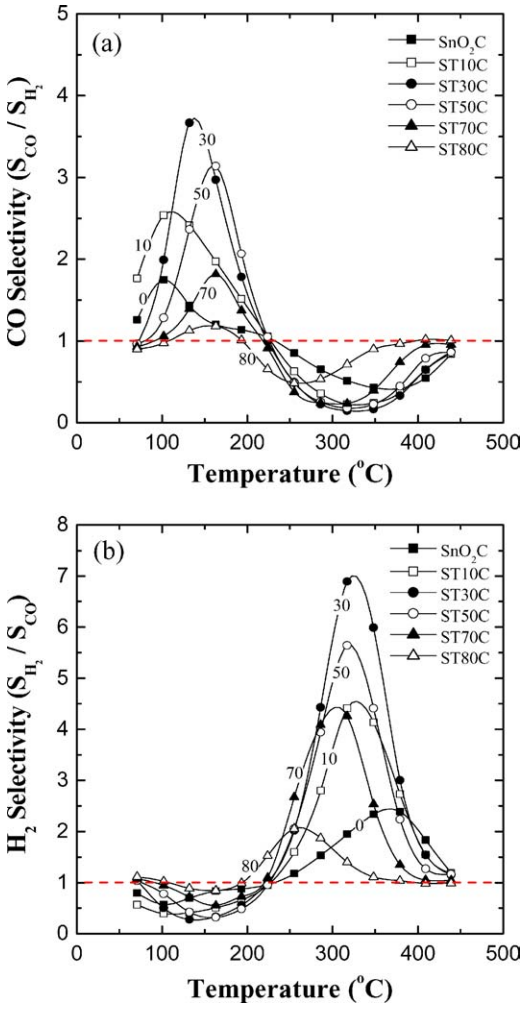

Fig. 8. (a) Temperature dependence of the CO-gas selectivity and (b) the H_2-gas selectivity for CuO-coated SnO_2-TiO_2 composites. The selectivity was defined as (a) the ratio of the CO sensitivity to the H_2 sensitivity or (b) vice versa.

to H_2 gas was relatively high. Above 70 mol% TiO_2, the sensitivity value to H_2 gas decreased below that of SnO_2C. Although the sensitivity value of CuO-coated SnO_2-TiO_2 composites to CO gas increased twice with CuO coating, the sensitivity value to H_2 gas did not show appreciable change.

Figure 8 shows the selectivity of SnO_2C and CuO-coated SnO_2-TiO_2 composites for (a) CO gas against H_2 gas, defined as the ratio of the CO gas sensitivity to the H_2 gas sensitivity and (b) H_2 gas against CO gas. Since the sensitivity value of TiO_2C was very small to 200 ppm CO or H_2 gas, TiO_2C sample was excluded in the selectivity curves. SnO_2C showed a small selectivity value (∼1.7) for CO gas at ∼100°C. As TiO_2 content increased up to 30 mol%, the selectivity for CO gas gradually increased. As TiO_2 content further increased, however, the selectivity values decreased. Thus, ST30C composition showed the highest selectivity (∼3.7 at ∼130°C) for CO gas among all samples due to its high sensitivity to CO gas at low temperature, as shown in Fig. 7. Since all samples showed the higher sensitivity values to H_2 gas than that to CO gas at high

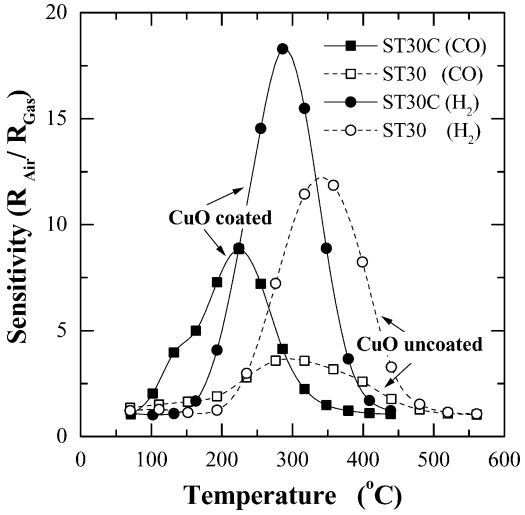

Fig. 9. Temperature dependence of the sensitivity of CuO-uncoated ST30 and CuO-coated ST30C to 200 ppm CO and 200 ppm H_2 gases.

temperature, the selectivity value for H_2 gas was nearly twice as high as that for CO gas for the same composition. Thus, ST30C composition also is the optimum composition for the selective detection of H_2 gas (∼6.9 at ∼315°C). The selectivity for CO gas was obtained in the temperature range between 100 and 190°C, however, the selectivity for H_2 gas was shown between 280 and 380°C, depending upon the TiO_2 content.

In order to show more clearly the effect of CuO coating for SnO_2-TiO_2 composites, the sensitivity curves for CuO-uncoated ST30 and CuO-coated ST30C to 200 ppm CO and 200 ppm H_2 gases were compared (Fig. 9). ST30 sample showed the large difference (∼45°C) in T_{MAX} between CO and H_2 gases due to the difference in sensing mechanism. With CuO coating, the T_{MAX} of ST30 for CO gas decreased from ∼295 to 225°C and the S_{MAX} to CO gas increased from ∼3.6 to ∼8.8. Similarly, the T_{MAX} of ST30 for H_2 gas decreased from ∼340 to ∼285°C and the S_{MAX} increased from ∼12.2 to ∼18.3. However, the CuO-coating increases the S_{MAX} to CO gas more than that to H_2 gas and decreases the T_{MAX} for CO gas more than that for H_2 gas. Thus, ST30C shows large difference in the T_{MAX} values between CO and H_2 gases while keeping high S_{MAX} value. As a result, ST30C showed the highest selectivity for CO gas at relatively low temperature (∼130°C) and the highest selectivity for H_2 gas at relatively high temperature (∼320°C), as shown in Fig. 8.

4. Conclusions

From the observation of the XRD patterns and the variation of lattice parameters, SnO_2 and TiO_2 forms a mixture when sintered at 800°C. In the uncoated system, the sensitivity of composites to H_2 gas was higher than that of SnO_2 due to the increased surface area below 80% TiO_2 addition, however, the sensitivity to CO gas of uncoated composites decreased from that of SnO_2.

The selectivity value of composite was modified with CuO coating and ST30C was found to be the optimum composition for the selective detection of either CO gas or H_2 gas. From the observation, the method to obtain the selective detection of CO gas was proposed. Controlling the temperature dependence of sensitivity value with composition and doping is a proposed method in this study.

References

1. P. Hauptmann, *Sensors; Principles and applications* (Prentice Hall, Salisbury, UK, 1991), pp. 115–124.
2. N. Yamazoe, Y. Kurokawa, and T. Seiyama, *Sensors and Actuators*, **4**, 283 (1983).
3. J.H. Yu and G.M. Choi, *Sensors and Actuators B*, **61**, 59 (1999).
4. J.H. Yu and G.M. Choi, *Sensors and Actuators B*, **52**, 251 (1998).
5. W.J. Moon, J.H. Yu, and G.M. Choi, *Sensors and Actuators B*, submitted.
6. W.J. Moon, J.H. Yu, and G.M. Choi, *Sensors and Actuators B*, **80**, 21 (2001).
7. J.H. Yu and G.M. Choi, *Sensors and Actuators B*, **75**, 56 (2001).
8. M. Ferroni, M.C. Carotta, V. Guidi, G. Martinelli, F. Ronconi, O. Richard, D. Van Dyck, and J. Van Landuyt, *Sensors and Actuators B*, **68**, 140 (2000).
9. M. Radecka, K. Zakrzewska, and M. Rekas, *Sensors and Actuators B*, **47**, 194 (1998).
10. M. Pechini, "Method of Preparing Lead and Alkaline-Earth Titanates and Niobates and Coating Method Using the Same to Form Capacitor," U.S.Pat. No. 3330697, July 11, (1967).
11. S.H. Baek, *Sensor Handbook*, (Seawha, Korea, 1990), pp. 458–464.
12. M. Park, T.E. Mitchell, and A.H. Heuer, *J. Am. Cer. Soc.*, **58** 43 (1975).
13. D. Garcia and D. Speidel, *J. Am. Ceram. Soc.*, **53**, 322 (1972).
14. D.H. Yoon, J.H. Yu, and G.M. Choi, *Sensors and Actuators B*, **46**, 15 (1998).